Reconfigurable Planar Three-Legged Parallel Manipulators

M. John D. Hayes

Department of Mechanical and Aerospace Engineering, Carleton University, Ottawa, ON K1S 5B6, Canada

Abstract A new class of reconfigurable planar three legged platforms is introduced. Kinematic mapping techniques are applied to solve the forward and inverse kinematic problems, and to visualize the reachable workspace of the platform. The results show that the new class of manipulator is viable from a kinematic modelling point of view.

1 Introduction

There has been great interest in reconfigurable mechanisms in recent years (see Yim et al., March 2007, and Shen et al., 2003). Of particular interest is their application to manufacturing and assembly. This is partly due to the observation that such devices can change their topology (Fisher et al., 2004), which enables obstacle avoidance and the ability to move in crowded workspaces, et c.. What appears to be missing in the body of literature is a planar three-legged parallel manipulator kinematic architecture capable of changing the configuration of its moving platform, thereby enabling the reshaping of its reachable workspace. Such a platform could have applications to terrestrial and space telescope lens polishing and reshaping (Klimas, 2009).

In this paper, a novel architecture for reconfigurable three legged planar platforms with three degrees of freedom (DOF) is presented for the first time. The architecture comprises three revolute-prismatic-revolute (RPR) legs where the distal end of each kinematic chain is connected to a distinct point on the moving platform, while the other end is connected to ground. The moving platform is manipulated by changing the lengths of each of the three active prismatic joints. Such a topologically symmetric platform is abbreviated as a 3-$R\underline{P}R$ platform. Reconfigurability is provided by three redundant active prismatic joints joining every adjacent pair of the distal ends of the three $R\underline{P}R$ chains, see Figure 1. These three connecting $R\underline{P}R$

chains essentially comprise the moving platform. When the length of one of the connecting $R\underline{P}R$ chains is varied, the configuration of the platform changes.

The change in the relative location of the platform attachment points changes the platform forward and inverse kinematics, as well as the shape of the reachable workspace. The three DOF provided by changing the relative locations of the platform attachments points are redundant, and are reserved exclusively for reconfiguring the platform. For the kinematic analysis presented in this paper, it is assumed that all prismatic pairs (P-pairs) are active, and can change length in a controlled manner. All remaining revolute pairs (R-pairs) are passive.

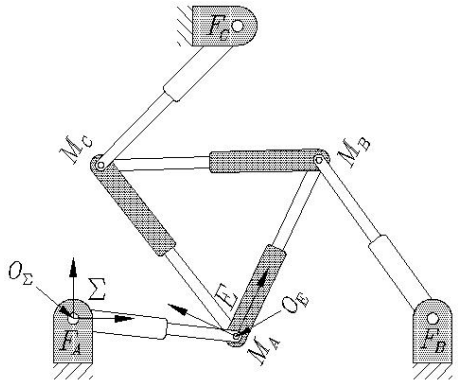

Figure 1. A reconfigurable planar three-legged platform.

The goals of this paper are to solve the forward and inverse position-level kinematic problems for such a platform, thereby demonstrating the viability of this class of platform from the perspective of kinematic modelling. The kinematic model developed by Hayes et al. (2004) will be adapted for this architecture. In addition, the reachable workspace envelope will be examined. This will be done by considering the limits of travel of each of the active P-pairs, and generating the workspace envelopes, adapting the techniques from Husty (1996) and Hayes (Oct. 2002).

2 The Forward And Inverse Kinematics Problem

Kinematic mapping may be used to compute the forward and inverse kinematics of reconfigurable 3-$R\underline{P}R$ planar platforms. While a very thorough discussion may be found in Bottema and Roth (1990), the essential idea is to

map the three homogeneous coordinates of the pole of a planar displacement to the points of a three dimensional projective image space.

Consider the reference frame E which can undergo general planar displacements relative to reference frame Σ, as illustrated in Figure 1. Let the homogeneous coordinates of points in the moving frame E be the ratios $(x : y : z)$, and homogeneous coordinates of the same point, but expressed in the fixed frame Σ, be the ratios $(X : Y : Z)$. The kinematic mapping image space coordinates are defined as:

$$\begin{aligned} X_1 &= a\sin(\varphi/2) - b\cos(\varphi/2); \quad X_2 = a\cos(\varphi/2) + b\sin(\varphi/2); \\ X_3 &= 2\sin(\varphi/2); \quad X_4 = 2\cos(\varphi/2); \end{aligned} \tag{1}$$

where a and b are the $(X/Z, Y/Z)$ Cartesian coordinates of the origin of E expressed in Σ, and φ is the orientation of E relative to Σ, respectively.

By virtue of the relationships expressed by Equations (1), the linear transformation that represents the basic group of planar Euclidean displacements of E with respect to Σ in terms of the image point is (Bottema and Roth, 1990)

$$\lambda \begin{bmatrix} X \\ Y \\ Z \end{bmatrix} = \begin{bmatrix} X_4^2 - X_3^2 & -2X_3X_4 & 2(X_1X_3 + X_2X_4) \\ 2X_3X_4 & X_4^2 - X_3^2 & 2(X_2X_3 - X_1X_4) \\ 0 & 0 & X_3^2 + X_4^2 \end{bmatrix} \begin{bmatrix} x \\ y \\ z \end{bmatrix}, \tag{2}$$

where λ is some non-zero constant arising from the use of homogeneous coordinates.

It has been shown (Hayes et al., 2004) that displacements of E relative to Σ in a planar 3-$R\underline{P}R$ platform map to the points of intersection of three quartics in X_i, each of which factors into two quadrics. The geometry of each $R\underline{P}R$ leg defines one of the quartics, having the following form:

$$\begin{aligned} &\big(K_0z^2(X_1^2 + X_2^2) + (-K_0x + K_1z)zX_1X_3 + (-K_0y + K_2z)zX_2X_3 \\ &-(K_0y + K_2z)zX_1X_4 + (K_0x + K_1z)zX_2X_4 - (K_1y - K_2x)zX_3X_4 \\ &\qquad +\tfrac{1}{4}[K_0(x^2 + y^2) - 2z(K_1x + K_2y) + K_3z^2]X_3^2 \\ &+\tfrac{1}{4}[K_0(x^2 + y^2) + 2z(K_1x + K_2y) + K_3z^2]X_4^2\big)\left(\tfrac{1}{4}(X_3^2 + X_4^2)\right) = 0. \end{aligned} \tag{3}$$

The *circle coordinates* (Hayes et al., 2004) which constrain the surface are $\mathbf{K} = [K_0 : K_1 : K_2 : K_3]$, and are artifacts of the geometry of each leg. The coordinate K_0 is an arbitrary homogenising constant, while $K_1 = -X_c$, $K_2 = -Y_c$, $K_3 = X_c^2 + Y_c^2 - r^2$, X_c and Y_c being the Cartesian coordinates of the centre of the ground fixed R-pair, and r is the length of the P-pair. The parameters X_c, Y_c, and r define a circle on which the centre of the distal R-pair must move.

The factor $1/4(X_3^2 + X_4^2)$ is exactly the non-zero condition of the planar kinematic mapping (Bottema and Roth, 1990), which must be satisfied for a point to be the image of a real displacement. Hence, this factor must be non-zero and may be safely divided out of the equation, leaving only the one quadric.

The set of three quadric constraint equations can always be simplified by setting $K_0 = X_4 = z = 1$ (Hayes and Husty, 2003) whereby the three quadrics take the form of three hyperboloids of one sheet when projected into the hyperplane $X_4 = 1$. These generally skew hyperboloids have the special property that they always have circular traces in planes parallel to $X_3 = 0$.

Moreover, the moving platform has a geometry defined by the locations of the vertices of the triangle determined by the three moving platform reference points, which in turn is defined by the lengths of the 3-$R\underline{P}R$ platform P-pairs. The forward kinematic problem can be stated as *given the lengths of the active P-pairs in each ground-fixed leg, and the lengths of the active P-pairs comprising the moving platform, what is the resulting position and orientation of the moving platform*? Solutions, if they exist, are the mutual intersections of the three constraint hyperboloids.

The inverse kinematic problem can be similarly stated as *given the position and orientation of the moving platform, together with its geometry, what are the lengths of the active P-pairs in each ground-fixed leg required to attain the specified pose*? Each leg can be considered separately because the solutions are decoupled from leg-to-leg. For any of the three legs, the distance between the fixed base point, F, and the moving platform point, M for that leg is the radius r of the constraint circle (the length of the P-pair, all other quantities being constants, see Figure 1. After setting $K_0 = X_4 = z = 1$, then substituting the coordinates of the image space point, $[X_1 : X_2 : X_3 : X_4]$, together with specified values for x, y, K_1, K_2, and K_3 into Equation (3), then expanding and collecting in terms of r yields a quadratic having the form:

$$Sr^2 + T = 0; \tag{4}$$

where

$$\begin{aligned} S &= -(X_3^4 + 1); \\ T &= 4(X_1^2 + X_2^2) + ((K_1^2 + K_2^2) - 2(K_1x + K_2y) + x^2 + y^2)X_3^2 + \\ &\quad (K_1^2 + K_2^2) + 2(K_1x + K_2y) + x^2 + y^2 + 4(K_1 - x)X_1X_3 - \\ &\quad (K_2 + y)X_1 + (K_2 - y)X_2X_3 + (K_1 + x)X_2 + (K_2x - K_1y)X_3. \end{aligned}$$

While this result means that there are two real solutions, only one is acceptable since the quantity represents the radius of a circle, which is, by convention, a positive non-zero number:

$$r = \left| \frac{\sqrt{-ST}}{S} \right|. \quad (5)$$

3 Workspace Boundary Visualization

The individual $R\underline{P}R$ leg lengths, r_i, must be within the joint limits $r_{i_{min}} \leq r_i \leq r_{i_{max}}$, where i denotes one of the legs in the set $\{A, B, C\}$. This condition means that for each leg there correspond two coaxial constraint hyperboloids. They bound the region of all possible positions and orientations of the platform, assuming the platform attachment points of the other two legs have been disconnected. Performing the same procedure for each leg in turn yields three solid regions bounded by six hyperboloids, each pair coaxial. The volume common to the six surfaces is the image of the reachable workspace for a particular set of platform edge lengths.

The active P-pairs on the moving platform change the relative locations of the platform attachment points in the moving frame E. This has the effect of translating the respective locations of the hyperboloid axes in the image space. Because the origin of E is on the platform attachment point of Leg A, the constraint hyperboloid axis of Leg A is invariant, whereas the axis locations for the other two legs can be manipulated. Regardless, the reachable workspace bounds are reshaped by changing the lengths of the active platform P-pairs.

4 Example

The following example illustrates: the forward and inverse kinematic solution procedures for arbitrary P-pair lengths within the ranges of travel of the three legs, and three platform edges; the effects of altering the geometry of the moving platform on the boundaries of the reachable workspace.

The goal in this first part is to solve the forward kinematic problem given arbitrary lengths of the three P-pair legs and three P-pair moving platform edges within finite bounds. Table 1 lists the ground-fixed R-pair centres expressed in Σ, the moving platform attachments expressed in E, the limits on the lengths of the base P-pairs, and the limits on the associated circle coordinates. An arbitrary set of leg lengths and platform edge lengths are listed in Table 2. These are the inputs to the forward kinematics problem.

Applying the algorithm described in Section 2 reveals that the three

constraint surfaces intersect in two real points. The two corresponding Cartesian poses of the platform, relative to Σ, are listed in Table 3, and illustrated in Figure 2.

Table 1. Manipulator kinematic geometry: fixed, minimum and maximum leg lengths and circle coordinates.

i	$F_{i/\Sigma}$	$M_{i/E}$ min	$M_{i/E}$ max	r_i min	r_i max	$\mathbf{K}_i$ min	$\mathbf{K}_i$ max
A	(0:0:1)	(0:0:1)	(0:0:1)	2	3	[1:0:0:-4]	[1:0:0:-9]
B	(4:0:1)	(2:0:1)	(3:0:1)	2	3	[1:-4:0:12]	[1:-4:0:7]
C	(2:4:1)	(1:$\sqrt{3}$:1)	($\frac{3}{2}$:$\frac{3}{2}\sqrt{3}$:1)	2	3	[1:-2:-4:16]	[1:-2:-4:11]

Table 2. Arbitrary kinematic geometry.

i	r_i	$M_{i/E}$
A	9/4	(0:0:1)
B	5/2	(9/4:0:1)
C	11/4	(1:7/4:1)

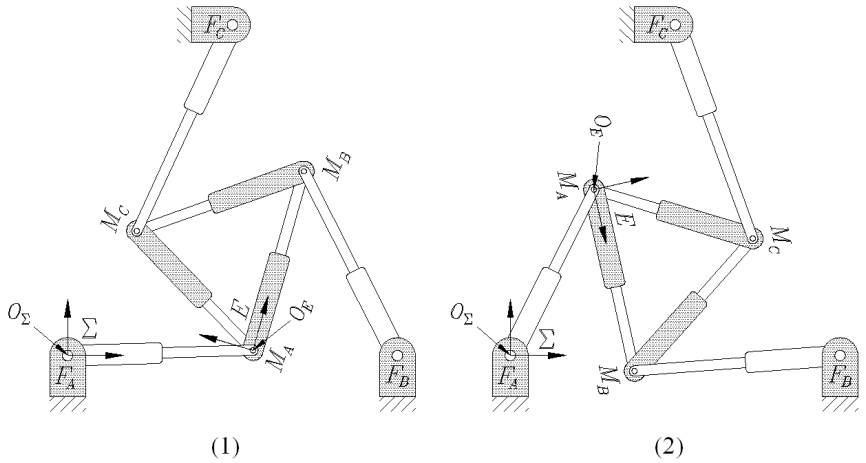

Figure 2. Two real solutions for the arbitrary geometry forward kinematic problem.

Next, the inverse kinematics problem is solved by determining the joint input value from the image point satisfying the associated constraint surface

Table 3. The two real solutions.

Solution	a	b	φ (deg.)
1	2.249073252	0.06457102532	74.07534341
2	1.014270872	2.008420726	-77.35021607

equation for each leg of the platform. When the two poses, the solutions to the forward kinematics problem, defined by a, b, and φ listed in Table 3 are mapped to X_1, X_2, and X_3, together with the appropriate fixed kinematic geometry listed in Table 1 are substituted into Equation (4), the result is exactly the inputs to the forward kinematics problem: the leg lengths listed in Table 2.

Finally, the effects of altering the geometry of the moving platform on the boundaries of the reachable workspace is addressed. The shape of the workspace is modified by changing the lengths of the three prismatic joints comprising the moving platform. For the kinematic geometry limits listed in Table 1, the corresponding bounding minimum and maximum hyperboloids are ilustrated in Figure 3.

Figure 3(a) illustrates the effects of changing the location of the platform attachment point for Leg C between it's minimum and maximum location in E. The axes of the two coaxial families of constraint hyperboloids are seen to be displaced. The total volume in common to the five sets of constraint hyperboloids is the kinematic mapping image of the reachable workspace. Cross-sections in the planes planes $X_3 = t$, where t is an arbitrary constant, reveal the reachable workspace at a particular orientation corresponding to $X_3 = t$.

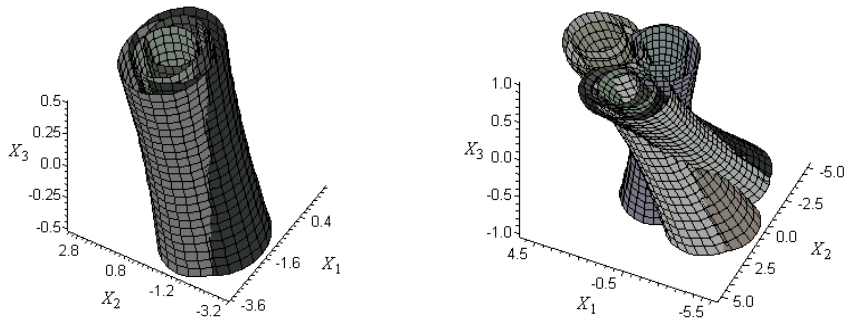

(a) Image of Leg C workspace.

(b) Image of platform workspace.

Figure 3. Kinematic image of the reachable workspace.

5 Conclusions

In this paper, a novel architecture for reconfigurable three legged planar platforms with three DOF has been presented for the first time. Reconfigurability is provided by three redundant active prismatic joints connecting every adjacent pair of distal ends of the three ground fixed $R\underline{P}R$ chains. The platform forward and inverse kinematics, as well as the effects of change in the relative location of the platform attachment points on the area of the reachable workspace have been illustrated with an example. These results demonstrate the kinematic feasibility of this class of reconfigurable three legged planar platform.

Bibliography

O. Bottema and B. Roth. *Theoretical Kinematics.* Dover Publications, Inc., New York, N.Y., U.S.A., 1990.

R. Fisher, R. P. Podhorodeski, and S. B. Nokleby. "Design of a Reconfigurable Planar Parallel Manipulator". *Journal of Robotic Systems*, vol. 21, no. 12: pages 665–675, 2004.

M.J.D. Hayes. "Architecture Independent Workspace Analysis of Planar Three-Legged Manipulators". *Proceedings of the WORKSHOP on Fundamental Issues and Future Research Directions for Parallel Mechanisms and Manipulators,* Québec, QC, Canada, pages 57–66, Oct. 2002.

M.J.D. Hayes and M.L. Husty. "On the Kinematic Constraint Surfaces of General Three-Legged Planar Robot Platforms". *Mechanism and Machine Theory*, vol. 38, no. 5: pages 379–394, 2003.

M.J.D. Hayes, P.J. Zsombor-Murray, and C. Chen. "Kinematic Analyais of General Planar Parallel Manipulators". *ASME, Journal of Mechanical Design*, 2004.

M.L. Husty. "On the Workspace of Planar Three-legged Platforms". *Proc. World Automation Conf., 6th Int. Symposium on Rob. and Manuf.* (ISRAM 1996), Montpellier, France, vol. 3: pages 339–344, 1996.

P. Klimas. "Research Possibilities into Mirror Polishing". *private communication,* (COM DEV Ottawa), 2009.

W.-M. Shen, P. Will, and B. Khoshnevis. "Self-Assembly in Space via Self-Reconfigurable Robots". *Multi-robot systems: from swarms to intelligent automata: proceedings from the 2003 International Workshop on Multi-Robot Systems edited by Alan C. Schultz, Lynne E. Parker, Frank E. Schneider*, pages 165–177, 2003.

M. Yim, W.-M. Shen, B. Salemi, D. Rus, M. Moll, H. Lipson, E. Klavins, and G.S. Chirikjian. "Modular Self-Reconfigurable Robot Systems: Challenges and Opportunities for the Future". *IEEE Robotics & Automation Magazine*, pages 43–52, March 2007.